

# Hopping Pilots for Estimation of Frequency-Offset and Multiantenna Channels in MIMO-OFDM

Xiaoli Ma, *Member, IEEE*, Mi-Kyung Oh, Georgios B. Giannakis, *Fellow, IEEE*, and Dong-Jo Park, *Member, IEEE*

**Abstract**—We design pilot-symbol-assisted modulation for carrier frequency offset (CFO) and channel estimation in orthogonal frequency-division multiplexing transmissions over multi-input multi-output frequency-selective fading channels. The CFO and channel-estimation tasks rely on null-subcarrier and nonzero pilot symbols that we insert and hop from block to block. Because we separate CFO and channel estimation from symbol detection, the novel training patterns lead to further decoupled CFO and channel estimators. The performance of our algorithms is investigated analytically, and then compared with an existing approach by simulations.

**Index Terms**—Carrier frequency offset (CFO), Cramér–Rao lower bound, frequency-selective channel, multi-input multi-output (MIMO)-orthogonal frequency-division multiplexing (OFDM), null subcarriers, pilot symbols.

## I. INTRODUCTION

ORTHOGONAL frequency-division multiplexing (OFDM) has been widely adopted by many standards (e.g., IEEE802.11a, IEEE802.11g in the U.S., and digital audio/video broadcasting (DAB/DVB), HiperLAN/2 in Europe), because it offers the possibility for high data rates at low decoding complexity [18], [23]. On the other hand, space–time multiplexing of multiantenna transmissions over multi-input multi-output (MIMO) channels has well-documented merits in combating fading, and further enhancing data rates (see, e.g., [17], [22], and references therein). For these reasons, MIMO-OFDM has emerged as a strong candidate for next-generation wireless multiantenna communications.

Implementing MIMO-OFDM however, faces two major challenges: 1) with the number of antennas increasing, channel

estimation becomes increasingly challenging as the number of unknowns increases; and 2) similar to single-antenna OFDM, MIMO-OFDM exhibits pronounced sensitivity to carrier frequency offset (CFO). A number of approaches have dealt with CFO and channel estimation in a single-input single-output (SISO) OFDM setup [1], [6], [10], [13], [15], [16]. Some rely on training blocks [12], [13], [21], while others just take advantage of the standardized transmission format; e.g., [6] and [10] exploit presence of null subcarriers. Recently, optimal training for MIMO channel estimation has been considered in [11] and [25], and preamble training for MIMO-OFDM has been proposed in [5], but CFO estimation was not taken into account. In the IEEE802.11a and HiperLAN/2 standards, sparsely placed pilot symbols are present in every OFDM symbol, and the pilot symbols are placed in the same positions from block to block. In this paper, we show how to place these training symbols across the blocks in order to effect estimation of both CFO and MIMO channels.

Different from the channel estimator in [11] and [25], we design the training patterns for estimating CFO and MIMO frequency-selective channels across several blocks. Unlike the space–time block-code-based iterative decoder for OFDM systems [7], we do not assume any specific space–time code, and our CFO-induced phase noise is allowed to change from symbol to symbol. Specifically, we design training symbols that enable decoupling of CFO and channel estimation from symbol decoding, which, in turn, leads to a low-complexity receiver, compared with blind and semiblind alternatives [3], [8], [24]. Moreover, our approach guarantees full acquisition range of the CFO estimator and identifiability of the MIMO channel estimator. Our scheme is also flexible to accommodate any space–time coded transmission.

The rest of the paper is organized as follows. In Section II, we begin with the description of the MIMO-OFDM system model. The CFO and channel estimators for MIMO-OFDM transceivers are derived in Section III. The Cramér–Rao lower bounds and performance analyses are given in Section IV. In Section V, simulation results demonstrate the potential of the novel algorithm, and Section VI concludes this paper.

*Notation:* Upper (lower) boldface letters will indicate matrices (column vectors). Superscript  $(\cdot)^H$  will denote Hermitian,  $(\cdot)^T$  transpose,  $(\cdot)^*$  conjugate, and  $\lfloor \cdot \rfloor$  will stand for the nearest integer. The real and imaginary parts are denoted as  $\Re[\cdot]$  and  $\Im[\cdot]$ ;  $E[\cdot]$  will stand for expectation, and  $\text{diag}[\mathbf{x}]$  for a diagonal matrix with  $\mathbf{x}$  on its main diagonal. Matrix  $\mathbf{D}_N(\mathbf{h})$  with a vector argument will denote an  $N \times N$  diagonal matrix with  $\mathbf{D}_N(\mathbf{h}) = \text{diag}[\mathbf{h}]$ . For a vector,  $\|\cdot\|$  denotes the Euclidean norm. We will use  $[\mathbf{A}]_{k,m}$  to denote the  $(k, m)$ th

Paper approved by R. Schober, the Editor for Detection, Equalization, and MIMO of the IEEE Communications Society. Manuscript received July 30, 2003. This paper was supported by collaborative participation in the Communications and Networks Consortium, sponsored by the U.S. Army Research Laboratory under the Collaborative Technology Alliance Program, Cooperative Agreement DAAD19-01-2-0011. The work of the first author was supported in part by the U.S. Army Research Office under Grant W911NF-04-1-0338. The U. S. Government is authorized to reproduce and distribute reprints for Government purposes notwithstanding any copyright notation thereon. This paper was presented in part at Globecom, San Francisco, CA, December 2003, and in part at the 37th Asilomar Conference on Signals, Systems, and Computers, Pacific Grove, CA, November 2003.

X. Ma is with the Department of Electrical and Computer Engineering, Auburn University, Auburn, AL 36849 USA (e-mail: xiaoli@eng.auburn.edu).

M.-K. Oh and D.-J. Park are with the Department of Electrical and Computer Science, Korea Advanced Institute of Science and Technology (KAIST), Daejeon 305-701, Republic of Korea (e-mail: ohmik@kaist.ac.kr; djpark@ee.kaist.ac.kr).

G. B. Giannakis is with the Department of Electrical and Computer Engineering, University of Minnesota, Minneapolis, MN 55455 USA (e-mail: georgios@ece.umn.edu).

Digital Object Identifier 10.1109/TCOMM.2004.840663

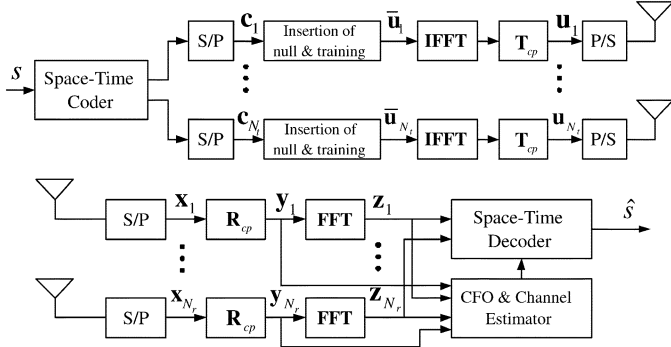


Fig. 1. Discrete-time-equivalent baseband model of MIMO block-transmission systems.

entry of a matrix  $\mathbf{A}$ , and  $[\mathbf{x}]_m$  for the  $m$ th entry of the column vector  $\mathbf{x}$ ;  $\mathbf{I}_N$  will denote the  $N \times N$  identity matrix;  $\mathbf{e}_i$  the  $(i + 1)$ st column of  $\mathbf{I}_N$ ;  $[\mathbf{F}_N]_{m,n} = N^{1/2} \exp(-j2\pi mn/N)$  the  $N \times N$  fast Fourier transform (FFT) matrix. We define  $\mathbf{f}_N(\omega) := [1, \exp(j\omega), \dots, \exp(j(N - 1)\omega)]^T$ .

## II. SYSTEM MODEL

Let us consider the discrete-time-equivalent baseband model of a block-transmission system communicating over MIMO frequency-selective channels in the presence of CFO, shown in Fig. 1. Suppose that every information symbol  $s(n)$  is drawn from a finite alphabet. Collecting  $N_s$  information symbols per information block, we denote the  $n$ th entry of the  $k$ th block as  $[\mathbf{s}(k)]_n = s(kN_s + n)$ . At the multiantenna transmitter, each block  $\mathbf{s}(k)$  is first encoded and/or multiplexed in space and time, to yield blocks  $\{\mathbf{c}_\mu(k)\}_{\mu=1}^{N_t}$  of length  $N_c$ . Training symbols (either zero or nonzero), known to both the transmitter and the receiver, are then inserted into  $\mathbf{c}_\mu(k)$  to form a vector  $\bar{\mathbf{u}}_\mu(k)$  with length  $N$ , for the  $\mu$ th antenna.

Following the insertion of training symbols, we just implement MIMO-OFDM. Specifically, we implement  $N$ -point inverse FFT (IFFT) (via left-multiplication with  $\mathbf{F}_N^H$ ) on each block  $\bar{\mathbf{u}}_\mu(k)$ , and insert the cyclic prefix (CP) (via left-multiplication with the appropriate matrix operator  $\mathbf{T}_{cp} := [\mathbf{I}_{L \times N}^T \mathbf{I}_N^T]^T$ , where  $\mathbf{I}_{L \times N}$  denotes the last  $L$  columns of  $\mathbf{I}_N$ ). After parallel-to-serial (P/S) conversion, the resulting blocks  $\{\mathbf{u}_\mu(k) = \mathbf{T}_{cp} \mathbf{F}_N^H \bar{\mathbf{u}}_\mu(k)\}_{\mu=1}^{N_t}$  of size  $P \times 1$  are transmitted through the  $N_t$  transmit antennas.

The  $L$ th-order frequency-selective channel from the  $\mu$ th transmit antenna to the  $\nu$ th receive antenna in discrete-time baseband-equivalent form is denoted by  $h^{(\nu,\mu)}(l)$ ,  $l \in [0, L]$ . These channels incorporate transmit (receive) filter  $g_\mu(t)$  ( $g_\nu(t)$ ) and the frequency-selective multipath  $g_{\nu,\mu}(t)$ ; i.e.,  $h^{(\nu,\mu)}(l) = (g_\mu \star g_{\nu,\mu} \star g_\nu)(t)|_{t=lT}$ , where  $\star$  denotes convolution, and  $T$  is the sampling period which is chosen equal to the symbol period. Let  $f_o$  be the frequency offset (in Hertz), which could be due to Doppler and/or mismatch between transmit–receive oscillators. In the presence of CFO, the samples at the  $\nu$ th receive antenna filter output can be written as

$$x_\nu(n) = e^{j\omega_o n} \sum_{\mu=1}^{N_t} \sum_{l=0}^L h^{(\nu,\mu)}(l) u_\mu(n-l) + \eta_\nu(n), \quad \nu \in [1, N_r] \quad (1)$$

where  $\omega_o := 2\pi f_o T$  is the normalized CFO, and  $\eta_\nu(n)$  is zero-mean, white, complex Gaussian distributed noise with variance  $\sigma_\eta^2$ . The sequence  $x_\nu(n)$  is then serial-to-parallel (S/P) converted into  $P \times 1$  blocks, with entries  $[\mathbf{x}_\nu(k)]_p := x_\nu(kP + p)$ . Selection of the block size  $P$  greater than the channel order  $L$  implies that each received block  $\mathbf{x}_\nu(k)$  depends only on two consecutive transmitted blocks,  $\mathbf{u}_\mu(k)$  and  $\mathbf{u}_\mu(k - 1)$ , which is referred to as interblock interference (IBI).

In order to remove IBI at the receiver, we discard the CP by left-multiplying  $\mathbf{x}_\nu(k)$  with the matrix  $\mathbf{R}_{cp} := [\mathbf{0}_{N \times L} \mathbf{I}_N]$ . Denoting the resulting IBI-free block as  $\mathbf{y}_\nu(k) := \mathbf{R}_{cp} \mathbf{x}_\nu(k)$ , we obtain the following vector-matrix input–output relationship for  $\nu \in [1, N_r]$ :

$$\mathbf{y}_\nu(k) = e^{j\omega_o kP} \sum_{\mu=1}^{N_t} \mathbf{R}_{cp} \mathbf{D}_P(\omega_o) \mathbf{H}^{(\nu,\mu)} \mathbf{T}_{cp} \mathbf{F}_N^H \bar{\mathbf{u}}_\mu(k) + \mathbf{R}_{cp} \boldsymbol{\eta}_\nu(k) \quad (2)$$

where  $\boldsymbol{\eta}_\nu(k) := [\eta_\nu(kP), \eta_\nu(kP + 1), \dots, \eta_\nu(kP + P - 1)]^T$ , with  $P = N + L$ ;  $\mathbf{H}^{(\nu,\mu)}$  is a  $P \times P$  lower triangular Toeplitz matrix with first column  $[h^{(\nu,\mu)}(0), \dots, h^{(\nu,\mu)}(L), 0, \dots, 0]^T$ ; and  $\mathbf{D}_P(\omega_o)$  is a diagonal matrix defined as  $\mathbf{D}_P(\omega_o) := \text{diag}[1, e^{j\omega_o}, \dots, e^{j\omega_o(P-1)}]$ .

Based on the structure of the matrices involved, it can be readily verified that  $\mathbf{R}_{cp} \mathbf{D}_P(\omega_o) = e^{j\omega_o L} \mathbf{D}_N(\omega_o) \mathbf{R}_{cp}$ , where  $\mathbf{D}_N(\omega_o) := \text{diag}[1, e^{j\omega_o}, \dots, e^{j\omega_o(N-1)}]$ . Following this identity, let us define  $\tilde{\mathbf{H}}^{(\nu,\mu)} := \mathbf{R}_{cp} \mathbf{H}^{(\nu,\mu)} \mathbf{T}_{cp}$ , where the  $N \times N$  matrix  $\tilde{\mathbf{H}}^{(\nu,\mu)}$  is circulant with first column  $[h^{(\nu,\mu)}(0), \dots, h^{(\nu,\mu)}(L), 0, \dots, 0]^T$ . Letting also  $\mathbf{v}_\nu(k) := \mathbf{R}_{cp} \boldsymbol{\eta}_\nu(k)$ , we can rewrite (2) as

$$\mathbf{y}_\nu(k) = e^{j\omega_o(kP+L)} \mathbf{D}_N(\omega_o) \sum_{\mu=1}^{N_t} \tilde{\mathbf{H}}^{(\nu,\mu)} \mathbf{F}_N^H \bar{\mathbf{u}}_\mu(k) + \mathbf{v}_\nu(k). \quad (3)$$

So far, our receiver-processing steps are the same as in any MIMO-OFDM system. In the *absence* of CFO, taking the FFT of  $\mathbf{y}_\nu(k)$  renders the frequency-selective channel equivalent to a set of flat-fading subchannels, since  $\mathbf{F}_N \tilde{\mathbf{H}}^{(\nu,\mu)} \mathbf{F}_N^H$  is a diagonal matrix  $\mathbf{D}_N(\tilde{\mathbf{h}}^{(\nu,\mu)})$ , where  $\tilde{\mathbf{h}}^{(\nu,\mu)} := [h^{(\nu,\mu)}(0), \dots, h^{(\nu,\mu)}(2\pi(N - 1)/N)]^T$ , with  $\tilde{h}^{(\nu,\mu)}(2\pi n/N) := \sum_{l=0}^L h^{(\nu,\mu)}(l) \exp(-j2\pi ln/N)$  denoting the  $(\nu, \mu)$ th channel's frequency-response values on the FFT grid. However, in the *presence* of CFO, the orthogonality among subcarriers is destroyed. And even if we perform the FFT at the receiver, the channel cannot be diagonalized. To simplify our input–output relationship, we insert  $\mathbf{F}_N^H \mathbf{F}_N = \mathbf{I}_N$  between  $\mathbf{D}_N(\omega_o)$  and  $\tilde{\mathbf{H}}^{(\nu,\mu)}$ , and re-express (3) as

$$\mathbf{y}_\nu(k) = e^{j\omega_o(kP+L)} \mathbf{D}_N(\omega_o) \sum_{\mu=1}^{N_t} \mathbf{F}_N^H \mathbf{D}_N(\tilde{\mathbf{h}}^{(\nu,\mu)}) \mathbf{F}_N \bar{\mathbf{u}}_\mu(k). \quad (4)$$

We deduce from (4) that estimating CFO and the multiple channels based on  $\{\mathbf{y}_\nu(k)\}_{\nu=1}^{N_r}$  is a nonlinear problem. Given  $\{\mathbf{y}_\nu(k)\}_{\nu=1}^{N_r}$ , our goal is to design training pilots for estimating the CFO  $\omega_o$  and the  $N_t N_r$  channels  $\tilde{\mathbf{h}}^{(\nu,\mu)} := [h^{(\nu,\mu)}(0), \dots, h^{(\nu,\mu)}(L)]^T$  in MIMO-OFDM systems.

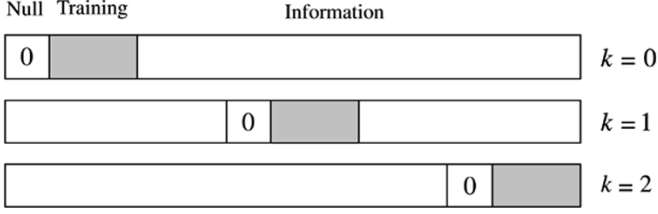


Fig. 2. One example of  $\tilde{\mathbf{u}}_\mu(k)$  structure.

### III. CFO AND CHANNEL ESTIMATION FOR MIMO-OFDM

Although  $\tilde{\mathbf{u}}_\mu(k)$  contains both information-bearing symbols and training symbols, their separation is challenging, due to the presence of CFO. In the following, we specify how to insert pilot symbols (both zero and nonzero ones), so that CFO estimation can be separated from MIMO channel estimation. The insertion of pilot symbols will be performed in two steps.

In the *first* step, we insert the pilot block  $\mathbf{b}_\mu(k)$  into the information-bearing block  $\mathbf{c}_\mu(k)$ , per transmit antenna, as follows:

$$\tilde{\mathbf{u}}_\mu(k) = \mathbf{P}_A \mathbf{c}_\mu(k) + \mathbf{P}_B \mathbf{b}_\mu(k) \quad (5)$$

where the two permutation matrices  $\mathbf{P}_A, \mathbf{P}_B$  have sizes  $K \times N_c$  and  $K \times N_b$ , respectively, and are selected to be mutually orthogonal:  $\mathbf{P}_A^T \mathbf{P}_B = \mathbf{0}_{N_c \times N_b}$ . Note that  $N_c + N_b = K$  and  $K < N$ . One example of such matrices is to form  $\mathbf{P}_A$  with the last  $N_c$  column of  $\mathbf{I}_{N_b+N_c}$ , and  $\mathbf{P}_B$  with the first  $N_b$  columns of  $\mathbf{I}_{N_b+N_c}$  for  $\mu \in [1, N_t]$ , given as

$$\mathbf{P}_A = [\mathbf{e}_{N_b} \ \cdots \ \mathbf{e}_{K-1}] \quad \text{and} \quad \mathbf{P}_B = [\mathbf{e}_0 \ \cdots \ \mathbf{e}_{N_b-1}]. \quad (6)$$

The structure of  $\tilde{\mathbf{u}}_\mu(k)$  in (5) is shown in Fig. 2. When  $\tilde{\mathbf{u}}_\mu(k)$  is left-multiplied by  $\mathbf{F}_N^H$ , the permutation matrices in (6) assign OFDM subcarriers to information and training symbols (pilot tones). We will specify the structure of the training block  $\mathbf{b}_\mu(k)$  later.

In the *second* step, we insert  $N - K$  zeros per block  $\tilde{\mathbf{u}}_\mu(k)$  to obtain  $\tilde{\mathbf{u}}_\mu(k)$ . This insertion can be implemented by left-multiplying  $\tilde{\mathbf{u}}_\mu(k)$ , with the null-subcarrier insertion matrix defined as

$$\mathbf{T}_{\text{sc}}(k) := [\mathbf{e}_{q_k(\text{mod}N)}, \dots, \mathbf{e}_{q_k+K-1(\text{mod}N)}] \quad (7)$$

where  $q_k := k \lfloor N/(L+1) \rfloor$ . We call each subcarrier corresponding to a zero symbol a null subcarrier. Dependence of the null-subcarrier insertion matrix  $\mathbf{T}_{\text{sc}}(k)$  on the block index  $k$  implies that the position of the inserted zero is changing from block to block. In other words, (7) implements a null-subcarrier hopping operation from block to block. Plugging (7) and (5) into (4), we deduce that the resulting signal at the  $\nu$ th receive antenna takes the following form:

$$\mathbf{y}_\nu(k) = e^{j\omega_o(kP+L)} \mathbf{D}_N(\omega_o) \mathbf{F}_N^H \sum_{\mu=1}^{N_t} \mathbf{D}_N(\tilde{\mathbf{h}}^{(\nu,\mu)}) \mathbf{T}_{\text{sc}}(k) \times [\mathbf{P}_A \mathbf{c}_\mu(k) + \mathbf{P}_B \mathbf{b}_\mu(k)] + \mathbf{v}_\nu(k). \quad (8)$$

We have described the insertion of two types of training symbols: zero and nonzero. We reiterate that the placement of the null pilot is hopping from block to block. In the following, we will show that this idea of hopping pilots is instrumental

in establishing identifiability of our CFO estimator, and achieving the minimum mean-square error of the MIMO channel estimator.

#### A. CFO Estimation

If the CFO was absent [ $\omega_o \equiv 0$  in (8)], then similar to [11] and [25], we could isolate from the received block the part corresponding to the training symbols, and by collecting several blocks (enough pilots), we could eventually estimate the channels. However, CFO destroys the orthogonality among subcarriers, and the training information is “mingled” with the unknown symbols and channels. This motivates acquiring the CFO first, and estimating the channels afterwards.

Our CFO estimation algorithm will rely on a “dehopping” operation, implemented on a per-block basis using the dehopping matrix

$$\mathbf{D}_N^H(k) := \text{diag} \left[ 1, e^{-j\frac{2\pi}{N} q_k}, \dots, e^{-j\frac{2\pi}{N} q_k(N-1)} \right]. \quad (9)$$

Because  $\mathbf{T}_{\text{sc}}(k)$  is a permutation matrix and  $\mathbf{D}_N(\tilde{\mathbf{h}}^{(\nu,\mu)})$  is a diagonal matrix, it is not difficult to verify that  $\mathbf{D}_N(\tilde{\mathbf{h}}^{(\nu,\mu)}) \mathbf{T}_{\text{sc}}(k) = \mathbf{T}_{\text{sc}}(k) \mathbf{D}_K(\tilde{\mathbf{h}}^{(\nu,\mu)}(k))$ , where  $\tilde{\mathbf{h}}^{(\nu,\mu)}(k)$  is formed by permuting the entries of  $\tilde{\mathbf{h}}^{(\nu,\mu)}$  as dictated by  $\mathbf{T}_{\text{sc}}(k)$ . Using the well-designed “dehopping” matrix in (9), it is easy to establish the identity

$$\mathbf{D}_N^H(k) \mathbf{F}_N^H \mathbf{T}_{\text{sc}}(k) = \mathbf{F}_N^H \mathbf{T}_{\text{zp}} \quad (10)$$

where  $\mathbf{T}_{\text{zp}} := [\mathbf{I}_K \ \mathbf{0}_{K \times (N-K)}]^T$  is a zero-padding operator. Multiplying (8) by the dehopping matrix, and using (10), we obtain

$$\tilde{\mathbf{y}}_\nu(k) = \mathbf{D}_N^H(k) \mathbf{y}_\nu(k) = e^{j\omega_o(kP+L)} \mathbf{D}_N(\omega_o) \mathbf{F}_N^H \mathbf{T}_{\text{zp}} \mathbf{g}_\nu(k) + \tilde{\mathbf{v}}_\nu(k) \quad (11)$$

where  $\mathbf{g}_\nu(k) := \sum_{\mu=1}^{N_t} \mathbf{D}_K(\tilde{\mathbf{h}}^{(\nu,\mu)}(k)) \tilde{\mathbf{u}}_\mu(k)$ , and  $\tilde{\mathbf{v}}_\nu(k) := \mathbf{D}_N^H(k) \mathbf{v}_\nu(k)$ . Equation (11) shows that after dehopping, null subcarriers in different blocks are at the same location, because  $\mathbf{T}_{\text{zp}}$  does not depend on the block index  $k$ . The system model (11), per receive antenna, is similar to the one used in [6] and [10] for the SISO-OFDM case. This observation suggests that we can generalize the method of [6] and [10] to estimate the CFO for MIMO-OFDM systems.

To this end, we consider the covariance matrix of  $\tilde{\mathbf{y}}_\nu(k)$  [cf. (11)]

$$\mathbf{R}_{\tilde{\mathbf{y}}_\nu} = \mathbf{D}_N(\omega_o) \mathbf{F}_N^H \mathbf{T}_{\text{zp}} E [\mathbf{g}_\nu(k) \mathbf{g}_\nu^H(k)] \times \mathbf{T}_{\text{zp}}^H \mathbf{F}_N \mathbf{D}_N^H(\omega_o) + \sigma_\eta^2 \mathbf{I}_N \quad (12)$$

where the noise  $\tilde{\mathbf{v}}_\nu(k)$  has covariance matrix  $\sigma_\eta^2 \mathbf{I}_N$ . In practice, supposing that the channels remain time-invariant during  $M$  blocks, we will replace the ensemble correlation matrix  $\mathbf{R}_{\tilde{\mathbf{y}}_\nu}$  by its sample estimate, formed by averaging across  $M$  blocks ( $M \geq K$ )

$$\hat{\mathbf{R}}_{\tilde{\mathbf{y}}_\nu} = \frac{1}{M} \sum_{k=0}^{M-1} \tilde{\mathbf{y}}_\nu(k) \tilde{\mathbf{y}}_\nu^H(k). \quad (13)$$

It has been shown in [10] that the column space of  $\hat{\mathbf{R}}_{\tilde{\mathbf{y}}_\nu}$  consists of two parts, the signal subspace and the null subspace. In the absence of CFO, if  $E[\mathbf{g}_\nu(k) \mathbf{g}_\nu^H(k)]$  has full rank, the

null space of  $\mathbf{R}_{\tilde{\mathbf{y}}_\nu}$  is spanned by the missing columns (the location of the null subcarriers) of the FFT matrix. The presence of CFO introduces a shift in the null space. Similar to [10], a cost function can be built to measure this CFO-induced shift for our MIMO-OFDM setup. With  $\omega$  denoting the candidate CFO, this cost function can be written as

$$J(\omega) := \sum_{n=K}^{N-1} \mathbf{f}_N^H \left( \frac{2\pi n}{N} \right) \mathbf{D}_N^{-1}(\omega) \left\{ \sum_{\nu=1}^{N_r} \mathbf{R}_{\tilde{\mathbf{y}}_\nu} \right\} \times \mathbf{D}_N(\omega) \mathbf{f}_N \left( \frac{2\pi n}{N} \right) \quad (14)$$

where  $\sum_{\nu=1}^{N_r} \mathbf{R}_{\tilde{\mathbf{y}}_\nu} = \mathbf{D}_N(\omega_o) \mathbf{F}_N^H \mathbf{T}_{\text{zp}} \left\{ \sum_{\nu=1}^{N_r} E[\mathbf{g}_\nu(k) \mathbf{g}_\nu^H(k)] \right\} \mathbf{T}_{\text{zp}}^H \mathbf{F}_N \mathbf{D}_N^H(\omega_o)$ . Clearly, if  $\omega = \omega_o$ , then  $\mathbf{D}_N(\omega_o - \omega) = \mathbf{I}_N$ . Next, recall that the matrix  $\mathbf{F}_N^H \mathbf{T}_{\text{zp}}$  is orthogonal to  $\left\{ \mathbf{f}_N(2\pi n/N) \right\}_{n=K}^{N-1}$ . Hence, if  $\omega = \omega_o$ , the cost function  $J(\omega_o)$  is zero in the absence of noise. However, we have to confirm that  $\omega_o$  is the unique minimum of  $J(\omega)$ . We will show that if  $\sum_{\nu=1}^{N_r} E[\mathbf{g}_\nu(k) \mathbf{g}_\nu^H(k)]$  has full rank, then  $\omega_o$  is indeed the unique zero of  $J(\omega)$ . To prove this, we establish the following proposition.

*Proposition 1:* If  $E[\mathbf{b}_\mu(k) \mathbf{b}_\mu^H(k)]$  is diagonal,  $\sum_{\mu=1}^{N_t} E[\mathbf{b}_\mu(k) \mathbf{b}_\mu^H(k)]$  has full rank,  $E[\mathbf{c}_{\mu_1}(k) \mathbf{c}_{\mu_2}^H(k)] = \mathbf{0}$ , and  $E[\mathbf{b}_{\mu_1}(k) \mathbf{b}_{\mu_2}^H(k)] = \mathbf{0}, \forall \mu_1 \neq \mu_2$ , then  $\sum_{\nu=1}^{N_r} E[\mathbf{g}_\nu(k) \mathbf{g}_\nu^H(k)]$  has full rank.

*Proof:* See Appendix A.

The conditions in *Proposition 1* seem unrelated to our estimation process and difficult to satisfy. Later, we will show that our training design for channel estimation satisfies these conditions. Using the result of *Proposition 1*, namely that  $\sum_{\nu=1}^{N_r} E[\mathbf{g}_\nu(k) \mathbf{g}_\nu^H(k)]$  has full rank, it follows readily that  $J(\omega) \geq J(\omega_o)$ , where the equality holds if and only if  $\omega = \omega_o$ . Therefore, CFO estimates can be found by minimizing  $J(\omega)$  as

$$\hat{\omega}_o = \arg \min_{\omega} J(\omega). \quad (15)$$

Thanks to subcarrier hopping,  $J(\omega)$  has a unique minimum in  $[-\pi, \pi)$ , regardless of the position of channel nulls. This establishes consistency of  $\hat{\omega}_o$ , and shows that the acquisition range of our CFO estimator in (15) is  $[-\pi, \pi)$ , which is the full range.

As the estimator in (15) requires line search, its complexity depends on the number of points searched over the interval  $[-\pi, \pi)$ . Similar to existing CFO estimators that enjoy a full acquisition range (e.g., the subspace-based ones in [10] and references therein), it is possible to reduce the complexity of  $\hat{\omega}_o$  in (15) in two ways: 1) restrict the full-range search if it is *a priori* known that the CFO lies in an interval smaller than  $[-\pi, \pi)$  (this is possible if a coarse CFO estimation algorithm has been applied as a preprocessor); or 2) avoid the search altogether by invoking a least-mean square (LMS) adaptive algorithm to search for the maximum of  $J(\omega)$  in (15). For details on the latter, we refer the reader to [10].

As usual, there are tradeoffs emerging among complexity, acquisition range, and variance of the CFO estimator in (15). The finer the search, the higher the complexity one incurs, but at the same time, the larger the acquisition range and/or lower estimator variance can be achieved. These tradeoffs are also present in existing CFO estimators; see, e.g., the one in [15], where acquisition range and variance improve relative to [21] at the price

of increasing complexity. Relative to [21] and [15] that estimate CFO in a closed form, the estimator in (15) has higher complexity. But as our simulations will also testify, it gains in acquisition range and has lower variance when the same overhead (rate) is used.

Going beyond the SISO CFO estimation problem, the estimator (15) in this paper will be combined with channel estimation in the ensuing section. More important, the main contributions here pertain to the MIMO and multiuser (broadcast) OFDM scenarios that have not been considered in, e.g., [10], [15], [16], or [21].

## B. Channel Estimation

Based on the estimated CFO in (15), we can remove the terms that depend on  $\omega_o$  from  $\{\tilde{\mathbf{y}}_\nu(k)\}_{k=0}^{M-1}$ , and proceed with channel estimation. To derive our MIMO channel estimator, we temporarily assume that the CFO estimate is perfect; i.e.,  $\hat{\omega}_o = \omega_o$ .

At the receiver, after removing the CFO-related terms from (11), we first take the FFT and then remove the null subcarriers by multiplying the blocks with  $\mathbf{T}_{\text{zp}}^T$  to obtain [cf. (5) and (11)]

$$\begin{aligned} \mathbf{z}_\nu(k) &= e^{-j\hat{\omega}_o(kP+L)} \mathbf{T}_{\text{zp}}^T \mathbf{F}_N \mathbf{D}_N^{-1}(\hat{\omega}_o) \tilde{\mathbf{y}}_\nu(k) \\ &= \sum_{\mu=1}^{N_t} \mathbf{D}_K(\tilde{\mathbf{h}}^{(\nu,\mu)}(k)) [\mathbf{P}_A \mathbf{c}_\mu(k) + \mathbf{P}_B \mathbf{b}_\mu(k)] + \xi_\nu(k) \end{aligned} \quad (16)$$

where  $\xi_\nu(k) := e^{-j\hat{\omega}_o(kP+L)} \mathbf{T}_{\text{zp}}^T \mathbf{F}_N \mathbf{D}_N^{-1}(\hat{\omega}_o) \tilde{\mathbf{v}}_\nu(k)$ . From the design of  $\mathbf{P}_A$  and  $\mathbf{P}_B$  in (6), we infer that  $\mathbf{P}_A^T \mathbf{D}_K(\tilde{\mathbf{h}}^{(\nu,\mu)}(k)) \cdot \mathbf{P}_B = \mathbf{0}$ . This allows us to decouple the training-based received symbols from the information-bearing symbols as

$$\begin{aligned} \mathbf{z}_{\nu,c}(k) &:= \mathbf{P}_A^T \mathbf{z}_\nu(k) \\ &= \sum_{\mu=1}^{N_t} \mathbf{P}_A^T \mathbf{D}_K(\tilde{\mathbf{h}}^{(\nu,\mu)}(k)) \mathbf{P}_A \mathbf{c}_\mu(k) + \xi_{\nu,c}(k), \\ \mathbf{z}_{\nu,b}(k) &:= \mathbf{P}_B^T \mathbf{z}_\nu(k) \\ &= \sum_{\mu=1}^{N_t} \mathbf{P}_B^T \mathbf{D}_K(\tilde{\mathbf{h}}^{(\nu,\mu)}(k)) \mathbf{P}_B \mathbf{b}_\mu(k) + \xi_{\nu,b}(k) \end{aligned} \quad (17)$$

where  $\xi_{\nu,c}(k) := \mathbf{P}_A^T(k) \xi_\nu(k)$ , and  $\xi_{\nu,b}(k) := \mathbf{P}_B^T(k) \xi_\nu(k)$ . By the definitions of  $\mathbf{P}_B$  in (6), and the dehopping matrix in (10), it follows that

$$\begin{aligned} \mathbf{D}_K(\tilde{\mathbf{h}}^{(\nu,\mu)}(k)) \mathbf{P}_B &= \mathbf{P}_B \mathbf{D}_{N_b}(\tilde{\mathbf{h}}_b^{(\nu,\mu)}(k)) \\ &= \mathbf{P}_B \text{diag}[\mathbf{F}(k) \mathbf{h}^{(\nu,\mu)}] \end{aligned} \quad (18)$$

where  $\tilde{\mathbf{h}}_b^{(\nu,\mu)}(k)$  contains the first  $N_b$  entries of  $\tilde{\mathbf{h}}^{(\nu,\mu)}(k)$ , the  $N_b \times (L+1)$  matrix  $\mathbf{F}(k)$  contains the first  $L+1$  columns and  $q_k$ -related  $N_b$  rows of  $\mathbf{F}_N$ , and  $\mathbf{h}^{(\nu,\mu)} := [h^{(\nu,\mu)}(0), \dots, h^{(\nu,\mu)}(L)]^T$ . Since  $\mathbf{P}_B^T \mathbf{P}_B = \mathbf{I}_{N_b}$ , we have

$$\mathbf{z}_{\nu,b}(k) = \sum_{\mu=1}^{N_t} \mathbf{B}_\mu(k) \mathbf{F}(k) \mathbf{h}^{(\nu,\mu)} + \xi_{\nu,b}(k) \quad (19)$$

where  $\mathbf{B}_\mu(k) := \text{diag}[\mathbf{b}_\mu(k)]$ . Note that unlike [11] and [25], the training-block length  $N_b$  for each block can be smaller than

$N_t(L+1)$ , by distributing training symbols across blocks. Collecting  $M$  blocks  $\mathbf{z}_{\nu,b}(k)$ , we can write the input–output relationship based on training symbols and channels as

$$\bar{\mathbf{z}}_{\nu,b} = \mathbf{B}\mathbf{h}_{\nu} + \bar{\boldsymbol{\xi}}_{\nu,b} \quad (20)$$

where  $\mathbf{h}_{\nu}$  consists of  $\{\mathbf{h}^{(\nu,\mu)}\}_{\mu=1}^{N_t}$ ,  $\bar{\boldsymbol{\xi}}_{\nu,b} := [\bar{\boldsymbol{\xi}}_{\nu,b}^T(0), \dots, \bar{\boldsymbol{\xi}}_{\nu,b}^T(M-1)]$  and

$$\mathbf{B} := \begin{bmatrix} \mathbf{B}_1(0)\mathbf{F}(0) & \cdots & \mathbf{B}_{N_t}(0)\mathbf{F}(0) \\ \vdots & \ddots & \vdots \\ \mathbf{B}_1(M-1)\mathbf{F}(M-1) & \cdots & \mathbf{B}_{N_t}(M-1)\mathbf{F}(M-1) \end{bmatrix}. \quad (21)$$

Notice that  $\mathbf{B}$  is the same  $\forall \nu \in [1, N_r]$ . Collecting  $\bar{\mathbf{z}}_{\nu,b}$ 's from all receive antennas into  $\bar{\mathbf{z}}_b := [\bar{\mathbf{z}}_{1,b}^T, \dots, \bar{\mathbf{z}}_{N_r,b}^T]^T$ , the linear minimum mean-square (LMMS) channel estimator is given by

$$\hat{\mathbf{h}}_{\text{LMMS}} := (\sigma^2 \mathbf{R}_h^{-1} + \mathbf{I}_{N_r} \otimes (\mathbf{B}^H \mathbf{B}))^{-1} (\mathbf{I}_{N_r} \otimes \mathbf{B}^H) \bar{\mathbf{z}}_b \quad (22)$$

where  $\mathbf{R}_h := E[\mathbf{h}\mathbf{h}^H]$  with  $\mathbf{h} := [\mathbf{h}_1^T, \dots, \mathbf{h}_{N_r}^T]^T$  is the channel covariance matrix, and  $\sigma^2$  denotes the noise variance.

Because  $\mathbf{R}_h$  is unknown in practice, the least-squares (LS) estimator can be used instead of the LMMS estimator, and with  $MN_b \geq N_t(L+1)$ , the matrix  $\mathbf{B}^H \mathbf{B}$  must be selected to have full rank. The LS channel estimator is given by

$$\hat{\mathbf{h}}_{\text{LS}} = (\mathbf{I}_{N_r} \otimes (\mathbf{B}^H \mathbf{B}))^{-1} (\mathbf{I}_{N_r} \otimes \mathbf{B}^H) \bar{\mathbf{z}}_b. \quad (23)$$

To guarantee that LS estimation can be performed, if the number of training symbols per block is  $N_b = N_t$ , we need a minimum number of  $M = L+1$  blocks, since we have  $\mathbf{h}^{(\nu,\mu)}$  with  $L+1$  entries to be estimated at the  $\nu$ th receive antenna.

The choice of  $\mathbf{b}_{\mu}(k)$ 's satisfying the conditions of *Proposition 1* is not unique. One possibility is to select  $N_b = N_t$ , and design the training sequences for different transmit antennas as

$$\mathbf{b}_{\mu}(k) = [\mathbf{0}_{\mu-1}^T \quad b \quad \mathbf{0}_{N_t-\mu}^T]^T, \quad \mu \in [1, N_t]. \quad (24)$$

Suppose  $N$  and  $M$  are integer multiples of  $L+1$ . Because our hopping step size is  $N/(L+1)$ , it can be verified that  $\mathbf{B}^H \mathbf{B}$  is a block diagonal matrix, given as

$$\begin{aligned} \mathbf{B}^H \mathbf{B} &= \text{diag} \left[ \sum_{m=0}^{M-1} \mathbf{F}^H(m) \mathbf{B}_1^H(m) \mathbf{B}_1(m) \mathbf{F}(m) \dots \right. \\ &\quad \left. \sum_{m=0}^{M-1} \mathbf{F}^H(m) \mathbf{B}_{N_t}^H(m) \mathbf{B}_{N_t}(m) \mathbf{F}(m) \right] \\ &= \frac{|b|^2 M}{N} \mathbf{I}_{N_t(L+1)}. \end{aligned}$$

The latter implies that increasing the number of blocks  $N$  improves channel-estimation performance. However, recall that this holds when the CFO estimator is perfect. Surprisingly, when CFO estimation is imperfect, the contrary is true. We should not use many blocks because the residual CFO estimation error degrades performance severely when the block index is large. In the following, we will describe a simple but necessary step to estimate the residual CFO.

### C. Phase Estimation

So far, we have estimated the CFO and the  $N_t N_r$  channels. For most schemes (e.g., [6], [10]), the CFO and channel estimation process ends here. However, this is not the case with our approach. We will show by simulations that the residual CFO will degrade the bit-error rate (BER) severely as the number of blocks increases. Therefore, one additional step is necessary to deal with the residual CFO. We will see that this step amounts to nothing but phase estimation.

After CFO compensation using the estimate in (15), the received block can be written as [cf. (11)]

$$\tilde{\mathbf{y}}_{\nu}(k) = e^{j(\hat{\omega}_o - \omega_o)(kP+L)} \mathbf{D}_N(\hat{\omega}_o - \omega_o) \mathbf{F}_N^H \mathbf{T}_{zP} \mathbf{g}_{\nu}(k) + \zeta_{\nu}(k) \quad (25)$$

where  $\hat{\omega}_o - \omega_o$  is the residual CFO, and  $\zeta_{\nu}(k) := e^{-j\hat{\omega}_o(kP+L)} \mathbf{D}_N^{-1}(\hat{\omega}_o) \mathbf{v}_{\nu}(k)$ . We observe from (25) that when the CFO estimate is accurate enough, the matrix  $\mathbf{D}_N(\hat{\omega}_o - \omega_o)$  can be approximated well by an identity matrix. However, the phase term  $(\hat{\omega}_o - \omega_o)(kP+L)$  becomes increasingly large as the block index  $k$  increases. Without mitigating it, the phase distortion degrades not only the performance of the channel estimator, but also the BER performance over time.

To enhance BER performance, we will use the nonzero training symbols to estimate the phase per block, which was originally designed for channel estimation. Suppose that for the  $k$ th block, we obtain the estimated channel from (21). Let us adopt the training sequence in (24) and suppose that the channel-estimation step is perfect. After equalizing the channel, for the  $\nu$ th antenna and the  $\mu$ th entry of  $\mathbf{z}_{\nu,b}(k)$ , the equivalent input–output relationship, provided that  $\mathbf{D}_N(\hat{\omega}_o - \omega_o) \approx \mathbf{I}_N$ , becomes

$$\phi_{\nu}(k) = e^{j(\hat{\omega}_o - \omega_o)(kP+L)} b + w_{\nu} \quad (26)$$

where  $\phi_{\nu}(k) := [\mathbf{z}_{\nu,b}(k)]_{\mu} / [\tilde{\mathbf{h}}_b^{(\nu,\mu)}(k)]_{\mu}$ , and  $w_{\nu}$  is the equivalent noise term after removing the channel. Since  $b$  is known, the phase  $(\hat{\omega}_o - \omega_o)(kP+L)$  can be estimated, based on the observations from  $N_r$  receive antennas on a per-block basis. To perform this phase-estimation step, we do not need to insert any additional pilot symbol, and the extra complexity is negligible. In Section V, we will verify that phase estimation improves performance markedly.

### D. Summary and Discussion

We have derived CFO and channel estimators for MIMO-OFDM systems. After removing the CFO and channels, the information symbols can be readily detected. In the following, we summarize our three-stage (CFO–channel–phase) estimation process in these steps.

- Step 1) Insert  $N_t$  training symbols in the information blocks  $\{\mathbf{c}_{\mu}(k)\}_{\mu=1}^{N_t}$  corresponding to the  $N_t$  transmit antennas, as shown in (24); the structure of  $\bar{\mathbf{u}}_{\mu}(k)$  is depicted in Fig. 2.
- Step 2) Insert one zero (one null subcarrier) per block whose position hops from block to block with hop-step  $N/(L+1)$ .
- Step 3) Perform the standard OFDM operations of IFFT and CP insertion per transmit antenna.

- Step 4) At the receiver, remove the CP first, and then dehop the received blocks to estimate  $\omega_o$  as in (15).
- Step 5) Compensate for the CFO, perform FFT, and remove null subcarriers.
- Step 6) Collect  $L + 1$  blocks, and estimate the channel as in (22).
- Step 7) Perform phase estimation to find the residual CFO per block.
- Step 8) Remove the residual CFO, and then detect the information symbols  $\mathbf{s}$ .<sup>1</sup>

The major advantages of our scheme are the following.

- Our training pattern matches well with that in IEEE802.11a and 11g, and the resulting algorithm has complexity affordable by current OFDM standards.
- Our scheme is flexible to adjust the training sequence, depending on the channel's coherence time and the pertinent burst duration; e.g., if the burst is long, we can insert fewer pilot symbols per block.
- Our transmission enjoys high spectral efficiency. Since  $N_t + 1$  training symbols are inserted every  $N + L$  transmitted symbols, our spectral efficiency is  $(N - N_t - 1)/(N + L)$ .
- Depending on the complexity that can be afforded, our estimators can be adjusted by collecting a variable number of blocks.
- Our CFO estimator has full acquisition range  $[-\pi, \pi)$ , while our channel estimator ensures identifiability at low complexity.
- Relative to existing alternatives [10], our CFO, channel, and phase estimators lead to improved BER performance. This will be confirmed by simulations in Section V.

Three remarks are now in order.

*Remark 1:* The algorithms we developed for estimating the single common CFO and the MIMO channel in our *single-user* setup, involving  $N_t$  transmit and  $N_r$  receive antennas, can be easily modified to estimate CFOs and channels in a *multiuser* downlink scenario, where the base station deploys  $N_t$  transmit antennas to broadcast OFDM-based transmissions to  $N_r$  mobile stations, each of which is equipped with a single antenna. In this case, we have  $N_r$  distinct CFOs and  $N_t N_r$  frequency-selective channels to estimate. However, each mobile station can still apply the CFO estimator in (15), using the cost function in (14) with  $N_r = 1$ . In addition, it is easy to verify that the LS channel estimator in (23) can be decoupled to estimate, on a per-receive-antenna basis, the  $N_t$  channel impulse responses contained in  $\mathbf{h}_\nu$  for  $\nu = 1, \dots, N_r$ .

*Remark 2:* Since it depends on the driving noise, the CFO generated by an oscillator's circuit is random in nature (see, e.g., [4, App. B] and references therein). Furthermore, the power of the phase noise in an oscillator is inversely proportional to the CFO range. This implies that a CFO estimation algorithm offering a larger acquisition range is useful on two counts: the outage probability of the CFO error is lower; and for the same oscillator hardware, the phase-noise power is lower.

*Remark 3:* Recalling that the null-subcarrier insertion matrix does not depend on the number of antennas, we deduce that our CFO estimator for MIMO-OFDM systems applies identically to a SISO-OFDM setup. This decoupling at the CFO estimation step can be implemented by training one antenna at a time. After compensating for the CFO, the same approach can be followed to estimate the MIMO channel using multiple SISO channel estimators. However, using existing training-based SISO CFO and separate SISO channel estimators to realize this one-antenna-at-a-time approach has the following limitations relative to our MIMO approach. The need emerges to switch between pilot- and information-transmission modes per antenna, which is more difficult to implement relative to our single-mode MIMO transmission format, and available SISO CFO estimators have a smaller acquisition range and require a coarse (in addition to a fine) CFO estimation step, which costs both in terms of complexity and spectral efficiency. The resultant bandwidth loss becomes severe in high-mobility applications where training has to be increasingly frequent. Furthermore, if a coarse estimation module is invoked to bring the CFO to a range manageable by, e.g., [15], then our full-range CFO estimator can also benefit from it to reduce the complexity of our search while still leading to improved error performance. Both limitations in complexity and spectral inefficiency are clearly illustrated in the broadcast-OFDM setup we discussed in *Remark 1*, where the one-antenna-at-a-time approach will be evidently inferior to this paper's approach by a factor proportional to the number of active users.

#### IV. PERFORMANCE ANALYSIS

To benchmark the performance of our estimators, we first derive the Cramér–Rao lower bounds (CRLB) for the CFO. Starting from the system model in (11), the CRLB for  $\omega_o$  is

$$\text{CRLB}_\omega = \left( \frac{2}{\sigma_v^2} \sum_{\nu=1}^{N_r} \sum_{k=0}^{M-1} \text{tr} \left[ \mathbf{D}(k) \mathbf{F}_N^H \mathbf{T}_{zP} \times \mathbf{R}_{gg}^{(\nu)} \mathbf{T}_{zP}^T \mathbf{F}_N \mathbf{D}(k) \right] \right)^{-1} \quad (27)$$

where  $\mathbf{D}(k) := \text{diag}[Pk + L, \dots, P(k + 1) - 1]$ , and  $\mathbf{R}_{gg}^{(\nu)} := E[\mathbf{g}_\nu(k) \mathbf{g}_\nu^H(k)]$ . It follows from (27) that as the number of blocks increases, the CRLB for CFO decreases. Similar comments apply for the signal-to-noise ratio (SNR) versus CRLB. If  $N \gg N - K$ , i.e., the number of subcarriers is much greater than the number of null subcarriers, we have that  $\mathbf{T}_{zP} \approx \mathbf{I}_N$ . Assuming that  $\mathbf{R}_{gg}^{(\nu)} = \mathcal{E} \mathbf{I}_N$ , where  $\mathcal{E}$  denotes the average symbol energy, and  $P, M$  are sufficiently large, we obtain

$$\text{CRLB}_\omega \approx \frac{\sigma_v^2}{\mathcal{E}} \frac{3}{2(P - L)P^2 M^3 N_r}. \quad (28)$$

As expected, the CRLB of CFO is independent of the channel and the number of transmit antennas, inversely proportional to the SNR, the number of receive antennas, and the cube of the number of space–time data.

<sup>1</sup>To further improve the performance, we can also update the channel estimation for the blocks after the first  $L + 1$  blocks.

TABLE I  
HIPERLAN/2 CHANNEL MODEL B

tap no.	0	1	2	3	4	5	6	7
var.	2.60e-01	2.44e-01	2.24e-01	7.07e-02	7.93e-02	4.78e-02	2.95e-02	1.78e-02
tap no.	8	9	10	11	12	13	14	15
var.	1.07e-02	6.45e-03	5.01e-03	2.51e-03	0	1.48e-03	0	6.02e-04

Assuming the CFO-estimation step is perfect, we can derive the performance of the channel estimator. If the LMMS channel estimator is adopted as in (22), then the mean-square error (MSE) of the channel estimator is given as

$$\sigma_{\text{lmms}}^2 = \text{tr} \left[ \left( \mathbf{R}_h^{-1} + \frac{M|b|^2}{N\sigma^2} \mathbf{I}_{N_t N_r (L+1)} \right)^{-1} \right]. \quad (29)$$

Similarly, if the LS estimator (23) is used, the corresponding MSE is given by

$$\sigma_{\text{ls}}^2 = \frac{N N_t N_r (L+1) \sigma^2}{M|b|^2}. \quad (30)$$

Both (29) and (30) imply that as the number of channels increases, the channel MSE increases. But this increase can be mitigated by collecting more blocks (i.e., more training symbols), provided that the CFO-estimation step is sufficiently accurate. Joint performance analysis goes beyond the scope of this paper.

## V. SIMULATIONS

We conduct simulations in various scenarios to verify the performance of our MIMO-OFDM designs. In all examples, the HiperLAN/2 channel model B is used to generate the channels. The channel order is  $L = 15$ , and the taps are independent with variances given in Table I. Unless otherwise specified, we design the OFDM block length  $N = 64$ , carrier frequency 5 GHz, and OFDM symbol (without CP) period  $3.2 \mu\text{s}$ , as in HiperLAN/2. The noise is additive white Gaussian with zero mean and variance  $\sigma_\eta^2$ . We define  $\text{SNR} = \mathcal{E}/\sigma_\eta^2$ , with  $\mathcal{E}$  denoting energy per symbol. The information symbols are drawn from a quaternary phase-shift keying (QPSK) constellation.

*Example 1 (Performance of CFO Estimator):* First, we test the effect of the number of blocks on CFO estimation when  $(N_t, N_r) = (2, 2)$ . The CFO is randomly selected in the range  $[0, 0.5\pi]$ . In each OFDM transmitted block, there are four nonzero pilot symbols, four zero symbols to remove interference from other channels, and one zero symbol serving as a null subcarrier. The placement of these pilot symbols follows the construction of Section III. Different numbers of blocks ( $M = L + 1, K, 2K$ , and  $3K$ ) are tested in this example. In Fig. 3, we depict the CFO normalized mean-square error (NMSE) defined as  $E[\|\hat{\omega}_o - \omega_o\|^2 / \|\omega_o\|^2]$  versus SNR. We observe that as the number of OFDM blocks  $M$  increases, the NMSE of CFO decreases. However, the improvement is relatively small, which suggests that using  $M = K$  OFDM blocks suffices to estimate the CFO. The CRLB we derived in Section IV is also shown as a bench mark in Fig. 3. The gap between the CFO NMSE and CRLB is indeed large.

We also test the effect of the number of antennas on CFO estimation. In Fig. 4, we plot the average NMSE of CFO when

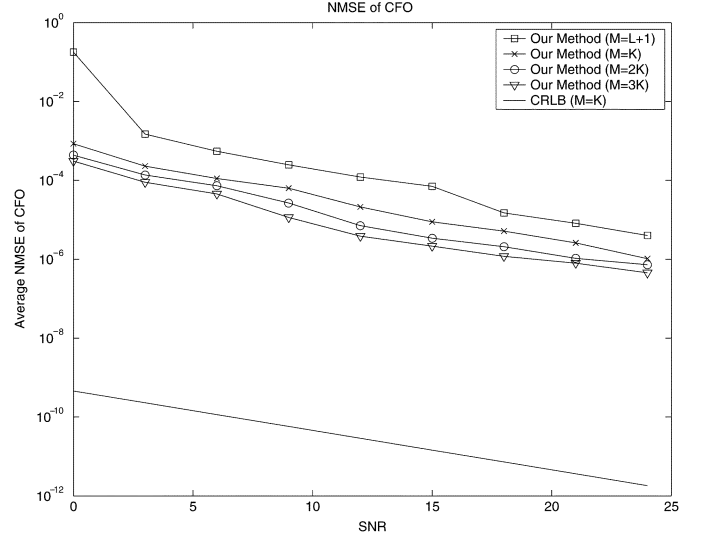


Fig. 3. Average CFO NMSE  $(N_t, N_r) = (2, 2)$ .

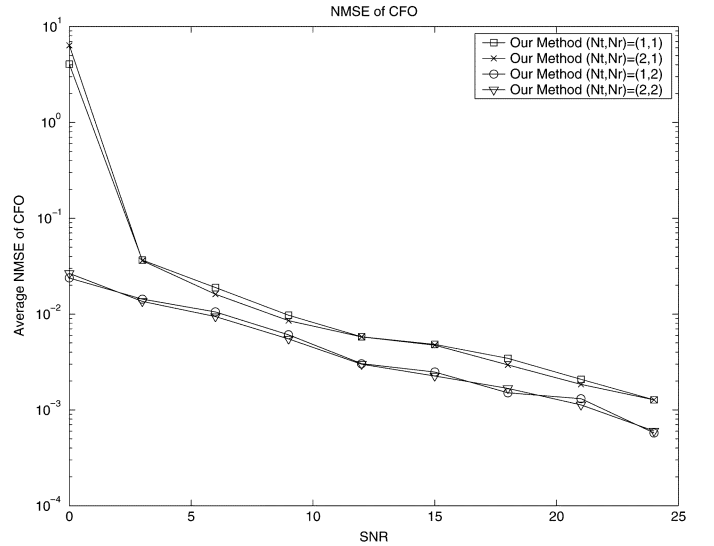
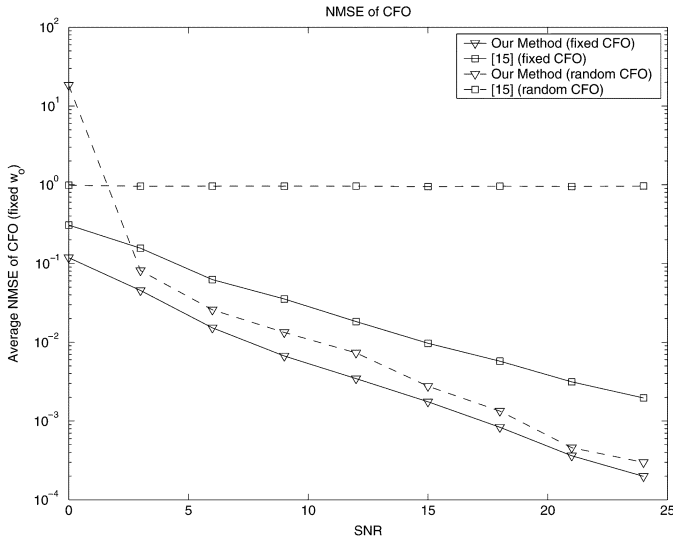


Fig. 4. Average CFO NMSE.

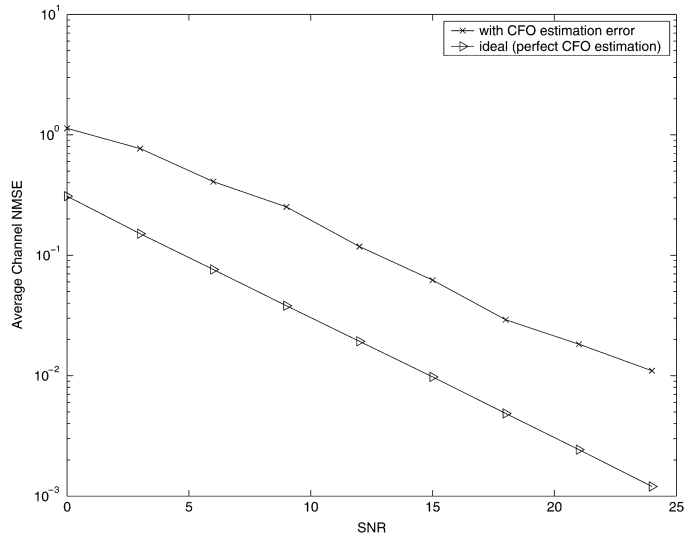
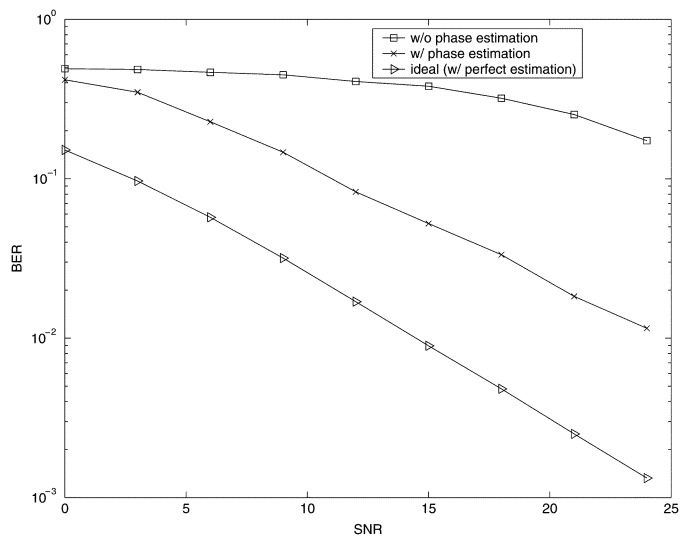
$(N_t, N_r) = (1, 1), (N_t, N_r) = (1, 2), (N_t, N_r) = (2, 1)$ , and  $(N_t, N_r) = (2, 2)$  with number of blocks  $M = N$ . For  $(N_t, N_r) = (1, 1)$  and  $(N_t, N_r) = (1, 2)$ , we use four nonzero pilot symbols and one null subcarrier per OFDM block. It is observed that as the number of receive antennas increases, the performance of CFO estimation improves, since the receive-diversity gain increases accordingly. Furthermore, note that the performance of CFO estimation does not depend on the number of transmit antennas. This is consistent with our performance analysis result.


 Fig. 5. Average CFO NMSE  $(N_t, N_r) = (1, 1)$ .

Next, we compare our method with the method in [15] for  $(N_t, N_r) = (1, 1)$ . For our method, we use one nonzero pilot and one zero pilot per block for a total of 64 blocks. To maintain the same transmission rate, the training block length of [15] is 128, with eight identical parts. Two cases are considered here: uniformly distributed CFO over  $[0, 0.5\pi]$ , and a fixed CFO  $\omega_o = \pi/128$ . For our method, we search over 2000 points equispaced within the range  $[0, \pi/16]$  for the fixed CFO case, and over  $[0, 0.5\pi]$  for the random case. From Fig. 5, we deduce that for a fixed CFO within the acquisition range of [15], our method outperforms the one in [15]. We also observe from Fig. 5 that when the CFO is uniformly distributed over  $[0, 0.5\pi]$ , our algorithm still enjoys performance comparable to the fixed CFO case, thanks to its large identifiability range; while the method in [15] suffers in performance because its acquisition range is only  $\omega_o \in [-\pi/16, \pi/16]$ .

As we discussed after (15), our CFO approach in the SISO case incurs higher complexity than the closed-form solution in [15], but gains in terms of lowering the estimator variance and enlarging the acquisition range. As we have explained in Remark 2, full-range CFO estimation is valuable to deal with outage probability effects of the random CFO [4, App. B]. Albeit more complex in estimating SISO CFO, our training sequence design has merits not only in combining CFO with channel estimation, but also in its scope that encompasses MIMO and multiuser (broadcast) OFDM settings.

*Example 2 (Performance of Channel Estimator):* In this example, we test the performance of MIMO channel estimation with  $(N_t, N_r) = (2, 2)$ , and CFO being also randomly selected in the range  $[0, 0.5\pi]$ . By collecting 64 observations which come from eight OFDM blocks, and using the LS channel estimator, we can estimate the MIMO channels. Fig. 6 depicts channel-estimation performance for MIMO-OFDM with estimated CFO. To measure channel-estimation quality, we compute the average channel NMSE as  $E[\|\hat{\mathbf{h}} - \mathbf{h}\|^2 / \|\mathbf{h}\|^2]$ , where  $\hat{\mathbf{h}}$  is obtained using the LS method. We compare with the “ideal case,” where the CFO is perfectly known. We note that there is 7-dB loss due to the CFO estimation error. This large gap suggests as a future topic CFO and MIMO channel estimation using iterative (a.k.a. turbo) techniques.


 Fig. 6. Average channel NMSE  $(N_t, N_r) = (2, 2)$ ,  $M = N$ .

 Fig. 7. BER  $(N_t, N_r) = (2, 2)$ ,  $M = N$ .

*Example 3 (BER Performance):* Since BER is the ultimate performance metric for communication systems, we plot BER versus SNR in Fig. 7. The simulation parameters are the same as the ones for Example 2. Zero-forcing equalization is used to estimate the information symbols. The ideal case corresponding to perfectly known channels and CFO is also shown as a benchmark. As discussed in Section III, BER performance degrades with the number of blocks due to residual CFO error. Fig. 7 shows the BER performance after mitigating the phase distortion, and corroborates our claim that the phase estimation improves BER performance considerably.

*Example 4 (Broadcast-OFDM):* Here we test the estimation of  $N_r$  CFOs in the multiuser broadcast-OFDM setup we described in Remark 1. In this simulation, we use  $(N_t, N_r) = (2, 2)$ , and CFOs randomly selected in the range  $[-0.5\pi, 0.5\pi]$ . Figs. 8 and 9 show the NMSE of our  $N_r \times 1$  vector CFO estimator and the resulting BER with phase estimation, which corroborate the merits of our method for broadcast-OFDM systems involving multiple CFOs.

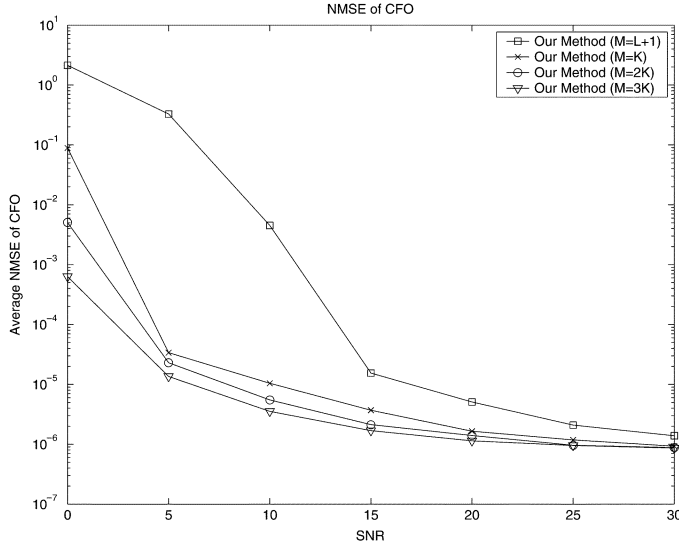


Fig. 8. Average CFO NMSE for MIMO-OFDM with  $N_r$  CFOs.

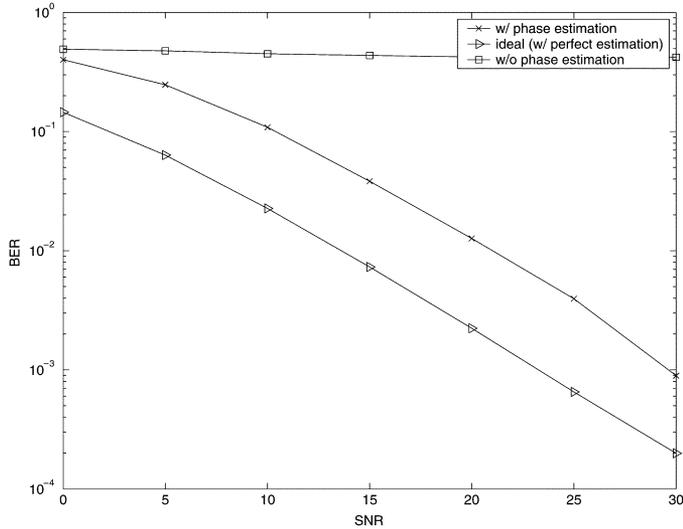


Fig. 9. BER performance with phase estimation with  $N_r$  CFOs.

## VI. CONCLUSION

In this paper, we derived algorithms to estimate the CFO and the channels in multiantenna OFDM transmissions. We have shown that at least one zero pilot per OFDM block for CFO estimation, and orthogonal training blocks of size  $N_t$ , are sufficient for MIMO channel estimation. Moreover, we proved that hopping pilots from block to block enlarges the CFO acquisition range to the full range, while inserting training symbols orthogonally per transmission block leads to low-complexity, high-performance channel estimation. Our training pattern is flexible, to be adjusted according to different standards, and is capable of achieving desirable complexity-performance tradeoffs. The performance of our estimators was benchmarked with CRLBs, investigated by simulations, and compared favorably with existing alternatives.

## APPENDIX A

### PROOF OF PROPOSITION 1

Based on (5) and the design constraint  $\mathbf{P}_A \mathbf{P}_B^T = \mathbf{0}$ , we obtain

$$\begin{aligned} E[\tilde{\mathbf{u}}_{\mu_1}(k) \tilde{\mathbf{u}}_{\mu_2}^H(k)] &= E[\mathbf{P}_A \mathbf{c}_{\mu_1}(k) \mathbf{c}_{\mu_2}^H(k) \mathbf{P}_A^T + \mathbf{P}_B \mathbf{b}_{\mu_1}(k) \mathbf{b}_{\mu_2}^H(k) \mathbf{P}_B^T] \\ &= \mathbf{0} \end{aligned} \quad (31)$$

for  $\mu_1 \neq \mu_2$ .

The expectation  $\sum_{\nu=1}^{N_r} E[\mathbf{g}_{\nu}(k) \mathbf{g}_{\nu}^H(k)]$  in (12) becomes

$$\begin{aligned} \sum_{\nu=1}^{N_r} E \left[ \left( \sum_{\mu_1=1}^{N_t} \mathbf{D}_K(\tilde{\mathbf{h}}_K^{(\nu, \mu_1)}(k)) \tilde{\mathbf{u}}_{\mu_1}(k) \right) \right. \\ \left. \times \left( \sum_{\mu_2=1}^{N_t} \tilde{\mathbf{u}}_{\mu_2}^H(k) \mathbf{D}_K^H(\tilde{\mathbf{h}}_K^{(\nu, \mu_2)}(k)) \right) \right] \\ = \sum_{\nu=1}^{N_r} \sum_{\mu=1}^{N_t} E \left[ \mathbf{D}_K(\tilde{\mathbf{h}}_K^{(\nu, \mu)}(k)) \tilde{\mathbf{u}}_{\mu}(k) \right. \\ \left. \times \tilde{\mathbf{u}}_{\mu}^H(k) \mathbf{D}_K^H(\tilde{\mathbf{h}}_K^{(\nu, \mu)}(k)) \right]. \end{aligned}$$

The matrix  $\bar{\mathbf{D}}_h^{(\nu, \mu)} := E[\mathbf{D}_K(\tilde{\mathbf{h}}_K^{(\nu, \mu)}(k))]$  has full rank by the design of our hopping pattern. Without loss of generality, selecting  $\mathbf{P}_A$  and  $\mathbf{P}_B$  as in (6), we obtain

$$\begin{aligned} \sum_{\nu=1}^{N_r} \sum_{\mu=1}^{N_t} E \left[ \mathbf{D}_K(\tilde{\mathbf{h}}_K^{(\nu, \mu)}(k)) \tilde{\mathbf{u}}_{\mu}(k) \tilde{\mathbf{u}}_{\mu}^H(k) \mathbf{D}_K^H(\tilde{\mathbf{h}}_K^{(\nu, \mu)}(k)) \right] \\ = \sum_{\nu=1}^{N_r} \sum_{\mu=1}^{N_t} \bar{\mathbf{D}}_h^{(\nu, \mu)} \left[ E \left[ \mathbf{b}_{\mu}(k) \mathbf{b}_{\mu}^H(k) \right] \mathbf{R}_c^{(\mu)} \right] \left( \bar{\mathbf{D}}_h^{(\nu, \mu)} \right)^H. \end{aligned}$$

Because  $\bar{\mathbf{D}}_h^{(\nu, \mu)}$  is diagonal, we can split it in two parts,  $\bar{\mathbf{D}}_{h,b}^{(\nu, \mu)}$  and  $\bar{\mathbf{D}}_{h,c}^{(\nu, \mu)}$ , with sizes  $N_b$  and  $N_c$ , respectively. To proceed with the proof, we recall the fact that the matrix  $\mathbf{A} + \mathbf{B}$  is positive definite, if matrices  $\mathbf{A}$  and  $\mathbf{B}$  are positive definite. Based on this, and because  $\mathbf{R}_c^{(\mu)}$  is positive definite, it follows that  $\sum_{\nu=1}^{N_r} \sum_{\mu=1}^{N_t} \bar{\mathbf{D}}_{h,c}^{(\nu, \mu)} \mathbf{R}_c^{(\mu)} (\bar{\mathbf{D}}_{h,c}^{(\nu, \mu)})^H$  is positive definite. According to the conditions in Proposition 1, we can verify that  $\sum_{\nu=1}^{N_r} \sum_{\mu=1}^{N_t} \bar{\mathbf{D}}_{h,b}^{(\nu, \mu)} E[\mathbf{b}_{\mu}(k) \mathbf{b}_{\mu}^H(k)] (\bar{\mathbf{D}}_{h,b}^{(\nu, \mu)})^H$  has full rank. It thus follows that  $\sum_{\nu=1}^{N_r} E[\mathbf{g}_{\nu}(k) \mathbf{g}_{\nu}^H(k)]$  has full rank. ■

## APPENDIX B

### CRLB FOR CFO ESTIMATOR

To derive the CRLB for CFO estimator, we start from the input-output relationship (11)

$$\mathbf{y}_{\nu}(k) = e^{j\omega_o(kP+L)} \mathbf{D}_N(\omega_o) \mathbf{F}_N^H \mathbf{T}_{zp} \mathbf{g}_{\nu}(k) + \bar{\mathbf{v}}_{\nu}(k). \quad (32)$$

Since the noise  $\bar{\mathbf{v}}_{\nu}(k)$  consists of zero-mean independent complex Gaussian distributed entries which are also independent from  $\mathbf{g}_{\nu}(k)$ , the joint probability density function of  $\mathbf{Y} := [\mathbf{y}_1(0), \dots, \mathbf{y}_1(M-1), \dots, \mathbf{y}_{N_r}(0), \dots, \mathbf{y}_{N_r}(M-1)]$  is given as

$$\begin{aligned} p(\mathbf{Y} | \omega_o, \mathbf{G}) = \frac{1}{(\pi \sigma_{\bar{\mathbf{v}}}^2)^{MN N_r}} \exp \left( -\frac{1}{\sigma_{\bar{\mathbf{v}}}^2} \sum_{\nu=1}^{N_r} \sum_{k=0}^{M-1} \left\| \mathbf{y}_{\nu}(k) \right. \right. \\ \left. \left. - e^{j\omega_o(kP+L)} \mathbf{D}_N(\omega_o) \mathbf{F}_N^H \mathbf{T}_{zp} \mathbf{g}_{\nu}(k) \right\|^2 \right) \end{aligned}$$

where  $\mathbf{G} := [\mathbf{g}_1(0), \dots, \mathbf{g}_1(M-1), \dots, \mathbf{g}_{N_r}(0), \dots, \mathbf{g}_{N_r}(M-1)]$ , and  $\sigma_v^2$  is the variance of one entry of  $\tilde{\mathbf{v}}_\nu(k)$ . Since  $\mathbf{T}_{zp}$  and  $\mathbf{F}_N^H$  are known, for  $M$  blocks of data, the log-likelihood function  $f(\omega_o, \mathbf{G})$  is (see [10] and [14])

$$\begin{aligned} f(\omega_o, \mathbf{G}) &= \ln p(\mathbf{Y}|\omega_o, \mathbf{G}) \\ &= -MNN_r \ln(\pi\sigma_v^2) - \frac{1}{\sigma_v^2} \sum_{\nu=1}^{N_r} \sum_{k=0}^{M-1} \left\| \mathbf{y}_\nu(k) \right. \\ &\quad \left. - e^{j\omega_o(kP+L)} \mathbf{D}_N(\omega_o) \mathbf{F}_N^H \mathbf{T}_{zp} \mathbf{g}_\nu(k) \right\|^2. \end{aligned} \quad (33)$$

The CRLB for CFO estimator is defined as

$$\text{CRLB}_\omega = \left( E \left[ \left| \frac{\partial f(\omega_o, \mathbf{G})}{\partial \omega_o} \right|^2 \right] \right)^{-1}. \quad (34)$$

Given  $f(\omega_o, \mathbf{G})$  as in (33), we obtain

$$\begin{aligned} \frac{\partial f(\omega_o, \mathbf{G})}{\partial \omega_o} &= -\frac{2}{\sigma_v^2} \sum_{\nu=1}^{N_r} \sum_{k=0}^{M-1} \Im \left( e^{j\omega_o(kP+L)} \tilde{\mathbf{v}}_\nu^H(k) \mathbf{D}(k) \right. \\ &\quad \left. \times \mathbf{D}_N(\omega_o) \mathbf{F}_N^H \mathbf{T}_{zp} \mathbf{g}_\nu(k) \right) \end{aligned}$$

where  $\mathbf{D}(k) := \text{diag}[Pk + L, \dots, P(k+1) - 1]$ . Thus, the Fisher information for the CFO estimator is given by

$$\begin{aligned} E \left[ \left| \frac{\partial f(\omega_o, \mathbf{G})}{\partial \omega_o} \right|^2 \right] &= \frac{2}{\sigma_v^2} \sum_{\nu=1}^{N_r} \sum_{k=0}^{M-1} \text{tr} \left[ \mathbf{D}(k) \mathbf{F}_N^H \mathbf{T}_{zp} \mathbf{R}_{gg}^{(\nu)} \right. \\ &\quad \left. \times \mathbf{T}_{zp}^T \mathbf{F}_N \mathbf{D}(k) \right] \end{aligned}$$

where  $\mathbf{R}_{gg}^{(\nu)} := E[\mathbf{g}_\nu(k) \mathbf{g}_\nu^H(k)]$ . The CFO CRLB is given by the inverse of the Fisher information.

## REFERENCES

- [1] J.-J. van de Beek, M. Sandell, and P. O. Börjesson, "ML estimation of time and frequency offset in OFDM systems," *IEEE Trans. Signal Process.*, vol. 45, pp. 1800–1805, Jul. 1997.
- [2] *Channel Models for HIPERLAN/2 in Different Indoor Scenarios Norme ETSI, Doc. 3ERI085B*, Eur. Telecommun. Standards Inst., 1998.
- [3] M. Ghogho and A. Swami, "Semi-blind frequency offset synchronization for OFDM," in *Proc. Int. Conf. Acoust., Speech, Signal Process.*, vol. 3, Orlando, FL, May 2002, pp. 2333–2336.
- [4] A. Hajimiri and T. H. Lee, *The Design of Low Noise Oscillators*. Norwell, MA: Kluwer, 1999.
- [5] Y. Li, "Simplified channel estimation for OFDM systems with multiple transmit antennas," *IEEE Trans. Wireless Commun.*, vol. 1, pp. 67–75, Jan. 2002.
- [6] H. Liu and U. Tureli, "A high-efficiency carrier estimator for OFDM communications," *IEEE Commun. Lett.*, vol. 2, pp. 104–106, Apr. 1998.
- [7] B. Lu, X. Wang, and Y. Li, "Iterative receivers for space-time block-coded OFDM systems in dispersive fading channels," *IEEE Trans. Wireless Commun.*, vol. 1, pp. 213–225, Apr. 2002.
- [8] M. Luise, M. Marselli, and R. Reggiannini, "Low-complexity blind carrier frequency recovery for OFDM signals over frequency-selective radio channels," *IEEE Trans. Commun.*, vol. 50, pp. 1182–1188, Jul. 2002.
- [9] X. Ma, G. B. Giannakis, and S. Ohno, "Optimal training for block transmissions over doubly-selective wireless fading channels," *IEEE Trans. Signal Process.*, vol. 51, pp. 1351–1366, May 2003.
- [10] X. Ma, C. Tepedelenlioglu, G. B. Giannakis, and S. Barbarossa, "Non-data-aided carrier offset estimations for OFDM with null subcarriers: Identifiability, algorithms, and performance," *IEEE J. Sel. Areas Commun.*, vol. 19, pp. 2504–2515, Dec. 2001.
- [11] X. Ma, L. Yang, and G. B. Giannakis, "Optimal training for MIMO frequency-selective fading channels," *IEEE Trans. Wireless Commun.*, to be published.
- [12] A. N. Mody and G. L. Stüber, "Synchronization for MIMO OFDM systems," in *Proc. IEEE Globecom*, vol. 1, San Antonio, TX, Nov. 2001, pp. 509–513.
- [13] P. H. Moose, "A technique for orthogonal frequency division multiplexing frequency offset correction," *IEEE Trans. Commun.*, vol. 42, pp. 2908–1314, Oct. 1994.
- [14] U. Mengali and A. D'Andrea, *Synchronization Techniques for Digital Receivers*. New York: Plenum, 1997.
- [15] M. Morelli and U. Mengali, "An improved frequency offset estimator for OFDM application," *IEEE Commun. Lett.*, vol. 3, pp. 75–77, Mar. 1999.
- [16] —, "Carrier-frequency estimation for transmissions over selective channels," *IEEE Trans. Commun.*, vol. 48, pp. 1580–1589, Sep. 2000.
- [17] A. F. Naguib, N. Seshadri, and R. Calderbank, "Increasing data rate over wireless channels," *IEEE Signal Process. Mag.*, vol. 17, pp. 76–92, May 2000.
- [18] R. Negi and J. Cioffi, "Pilot tone selection for channel estimation in a mobile OFDM system," *IEEE Trans. Consum. Electron.*, vol. 44, pp. 1122–1128, Aug. 1998.
- [19] M.-K. Oh, X. Ma, G. B. Giannakis, and D.-J. Park, "Cooperative synchronization and channel estimation in wireless sensor networks," in *Proc. 37th Asilomar Conf. Signals, Syst., Comput.*, Pacific Grove, CA, Nov. 2003, pp. 1084–1088.
- [20] J. G. Proakis, *Digital Communications*, 4th ed. New York: McGraw-Hill, 2000.
- [21] T. M. Schmidl and D. C. Cox, "Robust frequency and timing synchronization for OFDM," *IEEE Trans. Commun.*, vol. 45, pp. 1613–1621, Dec. 1997.
- [22] Q. Sun, D. C. Cox, and H. C. Huang, "Estimation of continuous flat fading MIMO channels," *IEEE Trans. Wireless Commun.*, vol. 1, pp. 549–553, Oct. 2002.
- [23] Z. Wang and G. B. Giannakis, "Wireless multicarrier communications: Where Fourier meets Shannon," *IEEE Signal Process. Mag.*, vol. 47, pp. 29–48, May 2000.
- [24] Y. Yao and G. B. Giannakis, "Blind carrier frequency offset estimation in SISO, MIMO, and multiuser OFDM systems," *IEEE Trans. Commun.*, to be published.
- [25] X. Ma, L. Yang, and G. B. Giannakis, "Optimal training for MIMO frequency-selective fading channels," in *Proc. 36th Asilomar Conf. Signals, Syst., Comput.*, Pacific Grove, CA, Nov. 2002, pp. 1107–1111.



**Xiaoli Ma** (M'03) received the B.S. degree in automatic control from Tsinghua University, Beijing, P.R. China, in 1998, and the M.Sc. and Ph.D. degrees in electrical engineering from the University of Virginia, Charlottesville, in 1999 and the University of Minnesota, Minneapolis, in 2003, respectively.

Since August 2003, she has been an Assistant Professor with the Department of Electrical and Computer Engineering, Auburn University, Auburn, AL. Her research interests include transmitter and receiver diversity techniques for wireless fading

channels, communications over time- and frequency-selective channels, complex-field and space-time coding, channel estimation and equalization algorithms, carrier-frequency synchronization for OFDM systems, and wireless sensor networks.



**Mi-Kyung Oh** received the B.S. degree from the Department of Electrical Engineering, Chung-Ang University, Seoul, Korea in 2000, and the M.S. degree in electrical engineering in 2002 from the Korea Advanced Institute of Science and Technology (KAIST), Daejeon, Korea, where she is currently working toward the Ph.D. degree.

From September 2002 to February 2004, she was a Visiting Researcher with the Department of Electrical and Computer Engineering, University of Minnesota, Minneapolis. Her research interests

include channel estimation, synchronization, ultra-wideband communications, and channel coding.



**Georgios B. Giannakis** (S'84–M'86–SM'91–F'97) received the Diploma in electrical engineering from the National Technical University of Athens, Greece, in 1981. He received the MSc. degree in electrical engineering in 1983, M.Sc. degree in mathematics in 1986, and the Ph.D. degree in electrical engineering in 1986, from the University of Southern California (USC), Los Angeles.

After lecturing for one year at USC, he joined the University of Virginia, Charlottesville, in 1987, where he became a Professor of Electrical Engineering in 1997. Since 1999, he has been with the University of Minnesota, Minneapolis, as a Professor in the Department of Electrical and Computer Engineering, and holds an ADC Chair in Wireless Telecommunications. His general interests span the areas of communications and signal processing, estimation and detection theory, time-series analysis, and system identification, subjects on which he has published more than 200 journal papers, 350 conference papers, and two edited books. Current research focuses on transmitter and receiver diversity techniques for single- and multiuser fading communication channels, complex-field and space-time coding, multicarrier, ultra-wideband wireless communication systems, cross-layer designs, and distributed sensor networks.

Dr. Giannakis is the corecipient of six Best Paper Awards from the IEEE Signal Processing (SP) Society (1992, 1998, 2000, 2001, 2003, and 2004). He also received the Society's Technical Achievement Award in 2000. He co-organized three IEEE-SP Workshops, and guest co-edited four special issues. He has served as Editor in Chief for the IEEE SIGNAL PROCESSING LETTERS, as Associate Editor for the IEEE TRANSACTIONS ON SIGNAL PROCESSING and the IEEE SIGNAL PROCESSING LETTERS, as secretary of the SP Conference Board, as member of the SP Publications Board, as member and vice-chair of the Statistical Signal and Array Processing Technical Committee, and as chair of the SP for Communications Technical Committee. He has served as a member of the Editorial Board for the PROCEEDINGS OF THE IEEE, and the steering committee of the IEEE TRANSACTIONS ON WIRELESS COMMUNICATIONS. He is a member of the IEEE Fellows Election Committee, and has served on the IEEE-SP Society's Board of Governors.



**Dong-Jo Park** (M'86) received the B.S. degree from the Department of Electrical Engineering, Seoul National University, Seoul, Korea in 1976, and the M.S. and Ph.D. degrees in electrical engineering from the University of California, Los Angeles, in 1981 and 1984, respectively.

He was a Senior Researcher with the Electronics and Telecommunications Research Institute (ETRI), Daejeon, Korea, from 1984 to 1985. He is currently a Professor with the Department of Electronic and Computer Science, Korea Advanced Institute of Science and Technology (KAIST), Daejeon, Korea. His research interests include multi-input multi-output systems, OFDM, multimedia signal processing, ultra-wideband communications, and channel coding.

Dr. Park is a member of IEICE, KIEE, KICS, and KISS.